Effect of Gold Oxide in Measurements of Colloidal Force

Rico F. Tabor,[†,⊥] Anthony J. Morfa,[‡,§] Franz Grieser,[§,⊥] Derek Y. C. Chan,[∥,⊥,#] and Raymond R. Dagastine*[,†,⊥]

[†]Department of Chemical and Biomolecular Engineering, University of Melbourne, Parkville 3010, Australia

[‡]Bio21 Institute, University of Melbourne, Parkville 3010, Australia

[§]School of Chemistry, University of Melbourne, Parkville 3010, Australia

[∥]Department of Applied Maths and Statistics, University of Melbourne, Parkville 3010, Australia

[⊥]Particulate Fluids Processing Centre, University of Melbourne, Parkville 3010, Australia

[#]Faculty of Life and Social Sciences, Swinburne University of Technology, Hawthorne, VIC 3122, Australia

ABSTRACT: Atomic force microscopy, contact-angle, and spectroscopic ellipsometry measurements were employed to investigate the presence and properties of gold oxide on the surface of gold metal. It was found that, in agreement with available literature, unoxidized gold surfaces were hydrophobic, whereas oxidation rendered the surface highly hydrophilic. The oxide could be removed with ethanol or base but appeared to be stable over long periods in water or salt solutions between pH 3 and 7. After oxidation, the oxide layer thickness, determined using ellipsometry, was consistent with an approximate monolayer of Au—O bonds at the gold surface. The presence of gold oxide was found to alter significantly the electrical double-layer characteristics of the gold surface below pH 6 and may explain the apparent inconsistencies in observed force behavior where gold is employed as well as aiding in design of future microfluidic systems which incorporate gold as a coating.
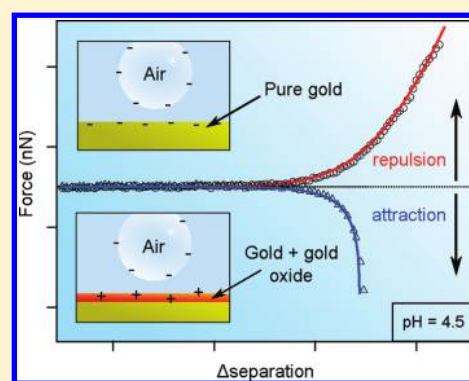
■ INTRODUCTION

Gold is an attractive material due to its high level of chemical inertness (nobility), high surface energy, and the fact that it can be generated as nanoparticles or easily deposited in thin layers (of a few nanometers or less). These properties have made it an important material in many areas of scientific research, particularly in surface and colloidal force measurements. It is often employed as a coating on silica or mica substrates to give a well-characterized, high-energy surface[1−4] that can be used as a support for self-assembled monolayers.[5,6] However, its reported properties still appear to vary significantly between studies, as the gold surface can be readily oxidized,[7] changing its chemical nature significantly. Additionally, because it is such a high-energy surface, it is very prone to contamination, which can leave doubt as to the purity of surfaces used in measurements.[2,8]

There has been a great deal of controversy about the wetting behavior of gold, with reports claiming either highly hydrophilic or hydrophobic "pure" gold surfaces.[7,9−11] The greater body of evidence suggested that the surface of pure gold is in fact hydrophobic but that it can be readily rendered hydrophilic by oxidation,[7] with trace water itself appearing to play a key role.[10] More recently, Stacchiola et al. demonstrated that water forms a locked bilayer on pure Au(111) surfaces, which is itself hydrophobic, as it has no exposed hydrogen-bonding sites,[12] supporting this theory. It has been shown that many of the standard laboratory cleaning procedures for generating highly pure surfaces for force measurements, particularly for use in the surface

force apparatus (SFA) and atomic force microscope (AFM), tend to generate oxide on gold.[7,13,14] Preparations such as cleaning in piranha solution (concentrated H_2O_2 and H_2SO_4), UV/ozone cleaning, and water or oxygen plasma cleaning all generate highly hydrophilic surfaces, suggesting the presence of gold oxide. Gold can also be readily oxidized by electrochemical methods,[15,16] that are of particular interest due to the use of gold in electrodes and electrochemical self-assembled monolayer (SAM) production.

There appears to be some discrepancy between force measurements involving gold surfaces, particularly when fitting the electrical double-layer behavior to understand surface charging in aqueous solutions. Wang and Yoon found the potential of gold in their AFM measurements to be around −56 mV in water (pH unspecified).[8] Giesbers et al. found that the zeta potentials and double-layer potentials of gold varied significantly with pH, exhibiting an isoelectric point at around pH 5 and a value of ≈−20 mV at pH 6−8.[17] The data of Barten et al. support these observations.[18] It is important to note that in all of these cases the possibility of oxide being present on the gold surface is mentioned, but their effects have not been quantified explicitly.

In this work, we use measurements of surface forces in order to better understand and explain the behavior of gold, particularly in the context of surface oxidation. Apparent ambiguities in

previous force measurements involving gold suggest that a study with well-characterized substrates is required, preferably employing a hydrophobic and nonoxidized probe. By using a bubble as a probe for surface forces, we make use of an interface which is by its nature hydrophobic and deformable and has well-characterized charging behavior,[19,20] allowing an accurate picture of the charging state of the gold surface to be obtained. Additionally, due to their ability to deform in response to applied forces, bubbles can increase their area of interaction with the gold surface as they approach, hence heightening the sensitivity of measurements of the electrical double-layer and other forces when compared to the solid probes used previously. We examine the effect of oxidation on the wettability and charging behavior of gold in water by measuring the force experienced when such bubble probes interact with these gold surfaces when in their pure (unoxidized) and oxidized states. Common laboratory "cleaning" procedures are employed in order to oxidize the gold surface, demonstrating that traditionally "clean" surfaces may in fact bear a layer of oxide. It is found that oxidation appears to move the isoelectric point (IEP) of the gold surface considerably as well as completely altering the wettability of the gold surface. These results serve to illustrate the important role of gold oxide, particularly in electrical double-layer formation, and may assist in interpretation of other force data for gold surfaces.

■ MATERIALS AND METHODS

Decanethiol was obtained from Sigma (Ultra-Grade) and used as received. Deionized water was from a Millipore Milli-Q system. Gold surfaces were prepared by sputter-coating 2 nm of chromium (as an adhesion promoter) followed by ≈40 nm of gold from an Au metal disk (99.999%) onto precleaned glass coverslips (Menzel-Gläser, 22 × 22 × 0.15 mm), using an Emitech K575x sputter coater. To produce oxidized gold surfaces, the coated coverslips were placed in a UV/ozone chamber (ProCleaner Plus, BioForce Nanoscience) and exposed for 20 min. Directly after oxidation, these surfaces exhibit complete wetting with water (contact angle ≈0°). Surfaces without oxide were prepared using two methods: either used directly from the sputter coater to minimize the possibility of any contamination or the ozone cleaning procedure was applied, followed by rinsing in absolute ethanol. This is known to remove oxide from the gold surface.[13] The resulting surface was tested for hydrophobicity by observing the contact angle of water to ensure that all oxide had been removed. Measurements employing both types of oxide-free surface were compared and found to give identical behavior. Roughness of the gold surfaces before and after oxidation was determined by AFM imaging studies to be consistently <0.5 nm rms. Solution pH was adjusted by addition of HNO_3 or NaOH solutions. Measurements of the water contact angle in air were made on a Dataphysics OCA tensiometer, using a syringe to grow drops of ≈100 μL in ≈20 μL increments. Contact angles for the growing drops were measured on either side of the drop and averaged over at least three measurements.

The optical properties of the gold surface were determined using spectroscopic ellipsometry. A Jobin-Yvon Horiba Uvisel ellipsometer was used to measure the ellipsometric values, Ψ and Δ, between 300 and 850 nm, in 5 nm steps, at a 70° angle of incidence. Using the J-Y DeltaPsi software, the optical properties of the system were modeled. This model consisted of a semi-infinite layer of gold (dielectric data from Aspnes et al.[21]) with a gold oxide layer (dielectric data from Kim et al.[22]) of varying thickness. The gold oxide film thickness was determined using the built-in DeltaPsi iterative fitting algorithm which minimizes the difference between the measured and predicted data.

Rectangular silicon AFM cantilevers (450 × 50 × 2 μm) were custom-made, with a circular gold pattern (diameter 45 μm, thickness ≈20 nm) added ≈5 μm from the end by focused ion-beam deposition.[23] This gold region was rendered hydrophobic by adsorption of decanethiol in ethanol (1 mM) for 2 h. Cantilever spring constants, K, were

determined by the method of Hutter and Bechhoeffer[24] and were in the range 0.10−0.15 N/m. The AFM measurements were performed on an Asylum MFP-3D AFM, equipped with a linear variable differential transformer (LVDT) sensor in the Z-movement direction, to allow direct detection of cantilever Z-position during force measurements. This has been shown to be vital for accurate force−displacement measurements, as the AFM piezo drive is not linear with input voltage to within our required tolerance.[25]

Bubbles were generated ultrasonically (Undatim Ultrasonics D-reactor), at a frequency of 515 kHz and power of 25 W.[26] The substrates used for bubble generation were glass Petri dishes that had been cleaned and then partially hydrophobized through a silano−ether coupling reaction in absolute ethanol for 2 h.[27] This was found to generate a surface of intermediate hydrophobicity (water contact angle 60°) which was appropriate for immobilizing bubbles, but which allowed them to be readily removed to the more hydrophobic patch on the cantilever. Bubbles used in these experiments were in the diameter range 80−140 μm.

In order to perform a measurement between a bubble and a gold surface, a bubble was picked up on a cantilever using the micropositioning stage of the AFM, so that it was attached to the hydrophobized gold patch on the cantilever. This allowed its contact area to be precisely known at all times, which proves vital for modeling purposes. A section of coverslip coated with the suitably prepared gold surface was then added to the Petri dish. The bubble was then brought over the gold surface, and the AFM was used to bring the bubble toward the surface at a low speed (200 nm/s) until a fixed deflection of the cantilever was reached, corresponding to around 40 nN. The deflection of the cantilever was measured by a laser and split photodiode, using the optical lever technique, and this deflection was converted to force using the cantilever spring constant and Hooke's law. Experiments were arranged and followed with high-magnification optical microscopy from below (Nikon TE2000, 40× objective). This allowed a precise measurement of bubble radii to be made to within ±2 μm. Once the gold surface had been introduced to the liquid, the experiment was performed as quickly as possible (<1 min) to minimize the potential for contamination, although no time-dependent behavior was noticed. Measuring the contact angle of water on the gold surface after the experiment showed no change, although the adsorption of inorganic ions could not be ruled out.

Experimental force vs separation data for bubble-gold approaches were predicted by using the Chan−Dagastine−White model. This model has been described in considerable detail previously[28−30] and hence will not be reproduced here. Briefly, this model couples expressions for the deformation and profile of the bubble to ones accounting for the disjoining pressure due to surface forces in the film region. By balancing these pressures, and assuming that the bubble maintains a constant volume and is incompressible[31] based on the diameter range used of ≈100−150 μm, both the deformation of the bubble and the potential of the surface can be deduced. It is also assumed the contact line of the bubble, corresponding to the perimeter of the gold patch on the cantilever, is pinned. For the data presented here, the only "free" or unconstrained parameter in the model is the surface potential of the gold. The other input parameters are the bubble radius (measured microscopically), bubble contact area (known explicitly by measuring the dimensions of the gold patch on the cantilever), retarded Hamaker function for air−water−gold (calculated using Lifshitz theory), Debye length (which was calculated from the solution pH and amount of acid/base added), and the surface potential of the bubble (which was determined in a previous study[19] and found to be in agreement with measurments obtained by Takahashi using microelectrophoresis[20]). Each measurement was repeated at least three times, and the surface potential was determined for each by comparing the experimental data with the theoretical prediction. The error bars on fitted values of the gold surface potentials show the confidence in the fitted value, incorporating tolerances within fitted parameters and error between measurements.

Table 1. Wetting Behaviour of Deionized Water on Gold Surfaces under Various Conditions before and after Oxidation[a]

sample	preparation conditions	contact angle
A	SC	84°
B	SC, OC	wet
C	SC, OC, EtOH	80°
D	SC, OC, H_2O (pH 7)	wet
E	SC, OC, H_2O (pH 3)	wet
F	SC, OC, H_2O (pH 11)	40°
G	SC, OC, 100 mM $NaClO_4$ (pH 7)	wet

[a] Samples C–G were stored in the noted solutions for 30 min, after which the surface was first dried under a stream of dry nitrogen before wetting experiments. SC = sputter coated, OC = treated in a UV/ozone chamber for 20 min. Note: "wet" refers to a state in which water spread to completely wet the surface and form a film.
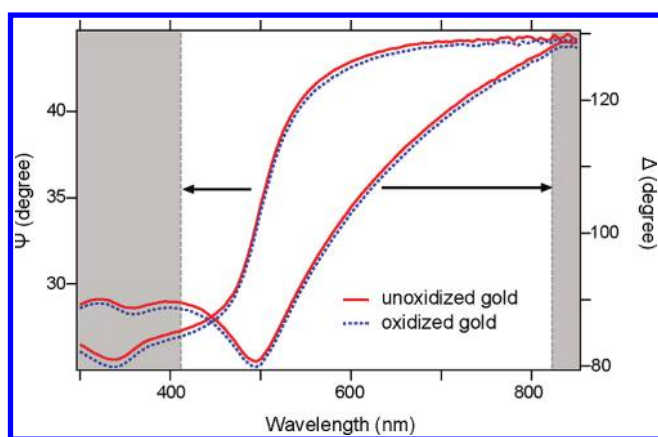
Figure 1. Measured spectroscopic ellipsometry data for gold films in air before (red, solid line) and after oxidation (blue, dashed line) plotted as a function of wavelength. The arrows indicate the axis against which the data are plotted, and the vertical dashed lines border the area between which the optical modeling was performed.

■ RESULTS AND DISCUSSION

The effect of oxidation on the hydrophobicity of gold was determined by measuring the contact angle of water on gold substrates before and after oxidation. In addition, the effect of typical solution conditions and cleaning methods was observed in order to test the stability of the oxide layer under the experimental conditions used. These results are summarized in Table 1.

These results are in agreement with available literature on the expected wetting state of the gold surface after similar preparation conditions,[7,32] and it has been demonstrated that ethanol is an effective reducing agent which removes the oxide layer from gold surfaces.[32] Gold oxide is also known to be soluble in strong base;[33] 30 min at pH 11 was not sufficient to completely reduce all of the oxide, although this treatment appeared to remove its coverage, as the surface returned to a partially hydrophobic state. The other solution treatments had no effect on the hydrophilicity of the gold, suggesting that in these conditions the oxide layer remained intact.

The presence of an oxide layer on the gold surface after oxidation, as suggested by wetting experiments, was further
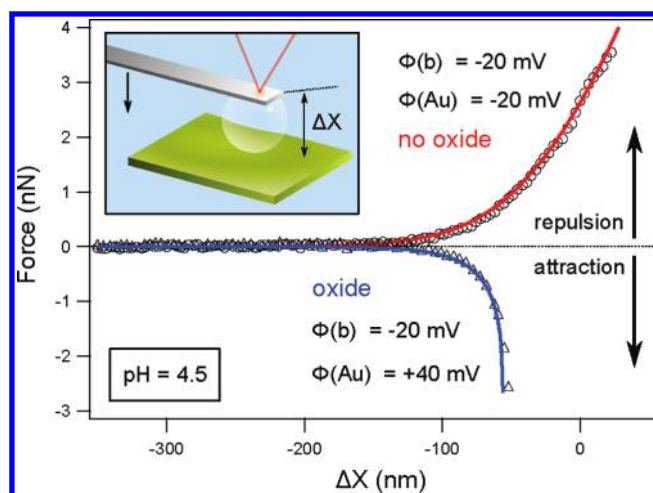
Figure 2. Force–displacement data measured by AFM between an air bubble and gold surface with and without surface oxide present at pH 4.5. Symbols are experimental data, and solid lines are the predicted interaction using the Chan–Dagastine–White model (see Materials and Methods section), fitted using the indicated surface potentials of the bubble, $\Phi(b)$, and gold surface $\Phi(Au)$. The value ΔX represents the separation between the end of the cantilever and the solid surface. The inset is a schematic representation of the experimental setup.

investigated using spectroscopic ellipsometry. Measurements were performed in air on gold samples before and after treatment with UV/ozone, and representative data from these experiments are shown in Figure 1. Spectroscopic ellipsometry measures the change in polarization and phase of polarized light upon reflection from a surface. The change in reflected amplitude and phase of the incident light are described by the Fresnel coefficients, that are determined by the dielectric function, ε, of the material, and are particularly sensitive to submonolayer coverages of materials.[34] Data are analyzed in the form of the two ellipsometric values, Δ and Ψ, that are related to the reflected amplitude of the s- and p-polarized states of light, r_s and r_p, respectively, by

$$\frac{r_p}{r_s} = \tan(\Psi)e^{i\Delta} \qquad (1)$$

Each measurement was optically modeled using dielectric data for gold and gold oxide in order to evaluate the contribution of each material to the measured values of Δ and Ψ. Modeling indicated that the initial (untreated) gold film had no gold oxide present and could be fitted with a semi-infinite gold model. Upon treatment with ozone, the measured Ψ and Δ values shifted to lower angles for a given wavelength, indicating a change in the dielectric properties of the gold surface, consistent with the growth of an oxide layer. Modeling the oxidized sample suggested a gold oxide layer with an average thickness of 1.8 Å was present, which is consistent with the observations of others.[22] The Au–O bonds in Au_2O_3 have been determined to be 2.0 Å,[35] and hence these results suggest an approximate monolayer of gold–oxygen bonds.

In order to determine the effect of oxidation of the gold surface on the electrical double-layer properties of gold in water, measurements were made between a bubble and gold surface as a function of pH, with no added background salt, but adjusted by addition of HNO_3 or NaOH. During close approach of the bubble and surface, assuming a net repulsion is present, the
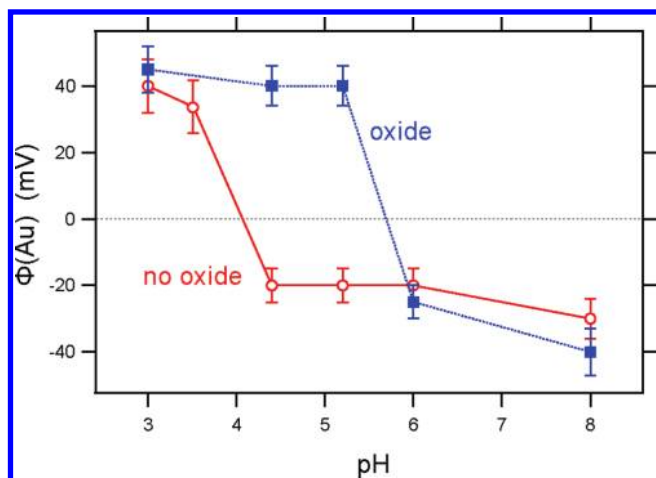
Figure 3. Apparent surface potentials, $\Phi(Au)$, of gold surfaces with (filled squares) and without (open circles) surface oxide present, obtained by model fits to experimental AFM interaction data between a bubble and gold surface. Bubble surface potentials were obtained previously,[19] and data were fit using the Chan—Dagastine—White model.[28]

disjoining pressure between the air—water and water—gold interfaces caused by electrical double-layer overlap and the van der Waals interaction causes the bubble to deform and flatten and a water film to form between bubble and surface. For the case of a net attractive pressure between the bubble and the surface, the resulting deformation of the air—water interface may result in coalescence of the bubble and surface. Because the bubble is able to deform in response to pressure caused by surface forces, for repulsive interactions, it becomes a much more sensitive probe to surface forces when compared with solid spheres which are traditionally used in AFM measurements of colloidal forces.

Interaction events between a bubble on the cantilever and the gold surface were measured in a variety of pH conditions. Sufficiently low approach speeds (200 nm/s) were used to give conditions in which hydrodynamics were negligible and could be omitted from the analysis.[23,29,30] These data were compared with predicted force curves, generated using the Chan—Dagastine—White model.[28—30] In order to account for the van der Waals interaction, a full retarded Hamaker function was calculated by the Lifshitz method, using spectral data for water from Dagastine et al.[36] and the dielectric construction for gold used optical data found in ref 37.

Figure 2 shows the interaction between a bubble and an oxidized or unoxidized gold surface at pH 4.5. For the unoxidized case, the interaction is repulsive, and hence a stable water film between the bubble and gold surface is generated. The magnitude and range of the repulsive force between the bubble and the surface suggest that the primary repulsion is due to overlap of electric double layers. The van der Waals force between a bubble and gold is strongly repulsive, tending to a Hamaker constant of -1.5×10^{-19} J at small separations. However, due to the effects of retardation, the force is still relatively short-ranged compared to the electrical double-layer interaction at low electrolyte concentration. Hence, it is clear that this repulsion is caused by overlap of electrical double layers, suggesting a negative charge on the gold surface at this pH. It has been previously postulated that this charge originates from adsorption of hydroxide ions.[38] For the oxidized case, there is a clear attraction between the

bubble and gold surface. Because the van der Waals interaction is always repulsive for this air—water—gold system, this attraction indicates an overlap of electrical double layers developed from oppositely charged surfaces. This suggests a difference in sign between the surface potential of the gold surface and air—water interface.

Similar measurements were made between bubbles and oxidized or unoxidized gold surfaces at a range of pH values to map the surface potential of the gold surfaces as a function of pH. Conditions above pH 8 were not used, as it may be expected that the gold oxide could become unstable over time,[33] and hence the surface would no longer be sufficiently well-characterized for these experiments. It can be seen in Figure 3 that there is a considerable difference between the apparent surface potential of the oxidized and unoxidized gold surfaces in the pH 3—6 region. Oxidation appears to move the apparent isoelectric point to a higher (more basic) pH value. The results for oxidized gold in this experiment are in agreement with the data presented by previous researchers,[17,18] who also found an isoelectric point at around pH 4.5—5. Although the oxidation state of their gold surfaces was not explicitly stated or measured, in both of those experiments surfaces were cleaned by either oxygen plasma or piranha solution, consistent with formation of an oxide layer on the gold.[14] Gold(III) oxide is known to be weakly acidic in hydrated form,[33] and hence it would be expected that the isoelectric point of the oxidized gold surface would move to a more basic value when compared to an unoxidized, pure gold surface. Interestingly, this may give additional opportunities for tuning self-assembly of organic molecules on gold surfaces, where the magnitude and sign of the surface potential are a key factor in determining the properties of the adsorbed/bonded layer.[32,39]

Because of the hydrophobic nature of the unoxidized gold surface, it may be expected for oxidized substrates that a short-range hydrophobic force[40] may operate at separations of a few nanometers to induce coalescence between the bubble and gold surface. In this experiment, such a force was not noted because the modeled data do not include points at separations where this could occur. For stable, repulsive interactions, the water film between the air—water and gold—water interfaces never became thin enough to enable such a short-range force to act. For interactions where the interfaces appeared to be oppositely charged, electrical double-layer forces acted at sufficiently large separations to give a strong attractive force at much greater film thicknesses. Hence, any very short-range attraction would be masked in the data. Some authors have noted a long-range, attractive force which acts between hydrophobic surfaces in water,[41] although the origin of this interaction is still disputed. It is important to note that in the experiments presented here the data could be readily and accurately predicted by solely by electrical double-layer interactions and the van der Waals force, and no evidence of a long-range hydrophobic force was apparent in the data.

■ CONCLUSION

It has been shown that despite its reputedly noble nature, the surface chemistry of gold is in fact quite complex and variable. Hydrophobic, pure gold surfaces are readily oxidized, and hence rendered hydrophilic, by common laboratory cleaning processes. Despite an apparent thickness of only around one Au—O bond length, the acidic oxide has a significant effect on the charging behavior of the gold surface with pH, giving a change in the

isoelectric point of around 2 pH units. The fact that surface oxidation and pH can be readily used to change the sign and potential of the gold surface suggest that these properties could be used to control self-assembly on gold surfaces and may be of particular interest when gold is used as an electrode. Hence, these results may aid understanding in experiments and design of systems which utilize gold, in both surface force and microfluidic fields.

■ REFERENCES

(1) Tabor, R. F.; Manica, R.; Chan, D. Y. C.; Grieser, F.; Dagastine, R. R. Repulsive van der Waals Forces in soft matter: Why bubbles do not stick to walls. *Phys. Rev. Lett.* **2011**, *106*, 064501/1–4.

(2) Ducker, W. A.; Senden, T. J.; Pashley, R. M. Measurements of forces in liquids using a force microscope. *Langmuir* **1992**, *8*, 1831–1836.

(3) Biggs, S.; Mulvaney, P. Measurement of the forces between gold surfaces in water by atomic force microscopy. *J. Chem. Phys.* **1994**, *100*, 8501–8505.

(4) Wall, J. F.; Grieser, F.; Zukoski, C. F. Monitoring Chemical Reactions at the Gold/Solution Interface Using Atomic Force Microscopy. *J. Chem. Soc., Faraday Trans.* **1997**, *93*, 4017–4020.

(5) Ruths, M.; Alcantar, N. A.; Israelachvili, J. N. Boundary friction of aromatic silane self-assembled monolayers measured with the surface forces apparatus and friction force microscopy. *J. Phys. Chem. B* **2003**, *107*, 11149–11157.

(6) Kane, V.; Mulvaney, P. Double-layer interactions between self-assembled monolayers of ÏL′-mercaptoundecanoic acid on gold surfaces. *Langmuir* **1998**, *14*, 3303–3311.

(7) White, M. L. The wetting of gold surfaces by water. *J. Phys. Chem.* **1964**, *68*, 3083–3085.

(8) Wang, J.; Yoon, R.-H. AFM forces measured between gold surfaces coated with self-assembled monolayers of 1-hexadecanethiol. *Langmuir* **2008**, *24*, 7889–7896.

(9) Smith, T. The Hydrophilic Nature of a Clean Gold Surface. *J. Colloid Interface Sci.* **1980**, *75*, 51–55.

(10) Erb, R. A. The Wettability of Gold. *J. Phys. Chem.* **1968**, *72*, 2412–2417.

(11) Gaines, G. L. On the Water Wettability of Gold. *J. Colloid Interface Sci.* **1981**, *79*, 295.

(12) Stacchiola, D.; Park, J. B.; Liu, P.; Ma, S.; Yang, F.; Starr, D. E.; Muller, E.; Sutter, P.; Hrbek, J. Water nucleation on gold: existence of a unique double-bilayer. *J. Phys. Chem. C* **2009**, *113*, 15102–15105.

(13) Ron, H.; Rubinstein, I. Self-assembled monolayers on oxidized metals. 3. alkylthiol and dialkyl disulfide assembly on gold under electrochemical conditions. *J. Am. Chem. Soc.* **1998**, *120*, 13444–13452.

(14) Tsai, H.; E., H.; Perng, K.; Chen, M.; Wu, J.-C.; Chang, Y.-S. Instability of gold oxide Au2O3. *Surf. Sci. Lett.* **2003**, *537*, L447–L450.

(15) Juodkazis, K.; Juodkazyte, J.; Jasulaitiene, V.; Lukinskas, A.; Sebeka, B. XPS studies on the gold oxide surface layer formation. *Electrochem. Commun.* **2000**, *2*, 503–507.

(16) Lohrengel, M. M.; Schultze, J. W. Electrochemical properties of anodic gold oxide layers-1: potentiostatic oxide growth and double layer capacity. *Electrochim. Acta* **1976**, *21*, 957–965.

(17) Giesbers, M.; Kleijn, J. M.; A., C. S. M. The electrical double layer on gold probed by electrokinetic and surface force measurements. *J. Colloid Interface Sci.* **2002**, *248*, 88–95.

(18) Barten, D.; Kleijn, J. M.; Duval, J.; van Leeuwen, H. P.; Lyklema, J.; Cohen Stuart, M. A. Double layer of a gold electrode probed by AFM force measurements. *Langmuir* **2003**, *19*, 1133–1139.

(19) Tabor, R. F.; Chan, D. Y. C.; Grieser, F.; Dagastine, R. R. Anomalous stability of carbon dioxide in pH-controlled bubble coalescence. *Angew. Chem., Int. Ed.* **2011**, *50*, 3454–3456.

(20) Takahashi, M. Zeta-potential of microbubbles in aqueous solutions: electrical properties of the gas-water interface. *J. Phys. Chem. B* **2005**, *109*, 21858–21864.

(21) Aspnes, D. E.; Kinsbron, E.; Bacon, D. D. Optical properties of Au: sample effects. *Phys. Rev. B* **1980**, *21*, 3290–3299.

(22) Kim, Y.-T.; Collins, R. W.; Vedam, K. Fast scanning spectro-electrochemical ellipsometry: in-situ characterisation of gold oxide. *Surf. Sci.* **1990**, *233*, 341–350.

(23) Vakarelski, I. U.; Manica, R.; Tang, X.; O'Shea, S. J.; Stevens, G. W.; Grieser, F.; Dagastine, R. R.; Chan, D. Y. C. Dynamic interactions between microbubbles in water. *Proc. Natl. Acad. Sci. U.S.A.* **2010**, *107*, 11177–11182.

(24) Hutter, J. L.; Bechhoefer, J. Calibration of atomic force microscope tips. *Rev. Sci. Instrum.* **1993**, *64*, 1868–1873.

(25) Manor, O.; Vakarelski, I. U.; Stevens, G. W.; Grieser, F.; Dagastine, R. R.; Chan, D. Y. C. Dynamic forces between bubbles and surfaces and hydrodynamic boundary conditions. *Langmuir* **2008**, *24*, 11533–11543.

(26) Vakarelski, I. U.; Lee, J.; Dagastine, R. R.; Chan, D. Y. C.; Stevens, G. W.; Grieser, F. Bubble Colloidal AFM Probes Formed from Ultrasonically Generated Bubbles. *Langmuir* **2008**, *24*, 603–605.

(27) Biggs, S.; Grieser, F. Atomic force microscopy imaging of thin films formed by hydrophobing reagents. *J. Colloid Interface Sci.* **1994**, *165*, 425–430.

(28) Chan, D. Y. C.; Dagastine, R. R.; White, L. R. Forces between a rigid probe particle and a liquid interface, I. The repulsive case. *J. Colloid Interface Sci.* **2001**, *236*, 141–154.

(29) Dagastine, R. R.; White, L. R. Forces between a rigid probe particle and a liquid interface, II. The general case. *J. Colloid Interface Sci.* **2002**, *247*, 310–320.

(30) Chan, D. Y. C.; Klaseboer, E.; Manica, R. Film drainage and coalescence between deformable drops and bubbles. *Soft Matter* **2011**, *7*, 2235–2264.

(31) Bhatt, D.; Newman, J.; Radke, C. J. Equilibrium force isotherms of a deformable bubble/drop interacting with a solid particle across a thin liquid film. *Langmuir* **2001**, *17*, 116–130.

(32) Ron, H.; Matlis, S.; Rubinstein, I. Self-assembled monolayers on oxidized metals. 2. gold surface oxidative pretreatment, monolayer properties, and depression formation. *Langmuir* **1998**, *14*, 1116–1121.

(33) Greenwood, N. N.; Earnshaw, A. *Chemistry of the Elements*, 2nd ed.; Butterworth-Heinemann: Oxford, 1997.

(34) Azzam, R. M. A.; Bashara, N. M. *Ellipsometry and Polarized Light*; North-Holland: Amsterdam, 1988.

(35) Jones, P. G.; Rumpel, H.; Schwartzmann, E.; Sheldrick, G. M.; Paulus, H. Gold(III) oxide. *Acta Crystallogr.* **1979**, *B35*, 1435–1437.

(36) Dagastine, R. R.; Prieve, D. C.; White, L. R. The dielectric function for water and its application to Van der Waals forces. *J. Colloid Interface Sci.* **2000**, *231*, 351–358.

(37) Palik, E. D. *Handbook of the Optical Constants of Solids*; Academic Press: Orlando, FL, 1985.

(38) Thompson, D. W.; Collins, I. R. Electrical Properties of the Gold-Aqueous Solution Interface. *J. Colloid Interface Sci.* **1992**, *152*, 197–204.

(39) Ron, H.; Rubinstein, I. Alkanethiol Monolayers on Preoxidized Gold. Encapsulation of Gold Oxide under an Organic Monolayer. *Langmuir* **1994**, *10*, 4566–4573.

(40) Van Oss, C. J. Long-range and short-range mechanisms of hydrophobic attraction and hydrophilic repulsion in specific and aspecific interactions. *J. Mol. Recognit.* **2003**, *16*, 177–190.

(41) Craig, V. S. J.; Ninham, B. W.; Pashley, R. M. Direct Measurement of Hydrophobic Forces: A Study of Dissolved Gas, Approach Rate, and Neutron Irradiation. *Langmuir* **1999**, *15*, 1562–1569.